Subspace projections to localise damage

A comparative model error robustness study

Muff, Daniel Vig; Ulriksen, Martin Dalgaard

[Link to publication from Aalborg University](#)

Subspace projections to localise damage: A comparative model error robustness study

Daniel V. Muff[1] and Martin D. Ulriksen[2]

1 Department of Civil Engineering, Aalborg University, Denmark, dvm1991@hotmail.com
2 Department of Civil Engineering, Aalborg University, Denmark, mdu@civil.aau.dk

Abstract

A model-based branch of damage localisation methods relates damage-induced changes in vibration signals to a theoretical model resembling the reference structure. One such method is the recently proposed Subspace Exclusion Zone (SEZ) scheme, whose methodological premise rests on the fact that a damage-induced shift in any field quantity, outside a closed boundary encompassing the damage, can be generated by stress fields acting on said boundary. Specifically, the interrogation procedure is to postulate one such boundary at a time, using a theoretical model, and then declare damage within the particular boundary that enables reconstruction of the damage-induced shifts. Needless to say, the SEZ scheme hinges on a sufficiently accurate model of the reference structure, as generally is the case for model-based approaches. To ascertain the SEZ scheme's robustness to model error, the present paper seeks a comparison to two other damage localisation schemes, namely, the Dynamic Damage Locating Vector (DDLV) and the Shaped Damage Locating Input Distribution (SDLID), which incorporate a theoretical model to, respectively, pinpoint damage by mapping forces to stresses and tailor controllable inputs to cancel the effect of damage. The robustness study is conducted in the context of numerical examples in which model errors are introduced.

1. Introduction

Vibration-based methods to successfully *detect* structural damage have reached a level of maturity at which practical application is feasible (1–4). The task of *locating* damage is, however, still considered a topic of academic research (5, 6), and methods exhibiting sufficient robustness for universal application have yet to emerge; despite the topic being given much research attention over the past fifty years (7). With that said, a multitude of schemes have been developed during this period, with some finding their own niche of applicability, as discussed by Fritzen in (8).

One of the factors responsible for the lack of robustness in existing localisation methods is the unfavourable ratio between modal parameter sensitivity to damage and sensitivity to other variabilities (6). The natural variability of modal parameters, related to environmental conditions, may well exceed that expected from damage; as shown by, for example, Farrar et. al (9), who conducted a study on a bridge that exhibited a 5 % variation of the first eigenfrequency during a 24 hour period due to environmental variability. As model-based damage

localisation schemes generally rely on a theoretical model to describe the reference structure, the aforementioned variation will undoubtedly cause errors in this model.

In the present paper, we examine the robustness to model errors of a recently proposed model-based localisation method, the Subspace Exclusion Zone (SEZ) scheme by Bernal and Ulriksen (10). This scheme locates damage in a forward manner by interrogating the domain from the boundaries of closed regions postulated in a model to contain the damage in their interior. As such, the SEZ scheme allows for a user-defined spatial localisation resolution and—when the loads in the reference and damaged states are proportional at the selected s-values in the Laplace domain—operates without calling for system identification. In order to gain a more general assessment of the scheme's model error robustness, we call on two other model-based schemes for comparison, namely, the Shaped Damage Locating Input Disctribution (SDLID) scheme by Ulriksen et. al (11), which utilises a theoretical model to shape inputs that may cancel the effect of damage, and the Dynamic Damage Locating Vector (DDLV) scheme by Bernal (12), in which a theoretical model is employed to compute a stress field pointing to the location of damage. The comparative study is conducted in the context of a numerical frame model introduced to model errors.

The remainder of this paper is structured as follows: Section 2 presents a condensed theoretical basis of the three schemes, limiting theory to only include that relevant to the paper. This is followed by a comparative study carried out in Section 3, where all three schemes are employed to locate damage in a frame model introduced to model errors. Finally, concluding remarks are expressed in Section 4.

2. Employed damage-localisation methods

The methods involved in the comparative study, namely, the SEZ, SDLID and DDLV schemes, all share the commonality of utilising a theoretical model. Be it to reproduce a shift in a kinematic field quantity, shape controllable inputs or generate a stress field, a sufficiently accurate model representation of the reference system is demanded by the schemes to operate as intended. In order for this paper to be self-contained, the following subsections provide a concise description of the theoretical foundation for each scheme, while more comprehensive coverage is available in (6, 10–12).

2.1 The SEZ scheme

The principle of the SEZ scheme rests on the fact that a damage-induced change in a given field quantity, outside a boundary, $\mathcal{B}$, enclosing the damage, may be replicated by applying stress fields on that boundary. If we consider a linear and time invariant (LTI), perturbed structural domain, $\mathcal{A} = \mathcal{A}_H \cup \mathcal{A}_D$—where $\mathcal{A}_H$ and $\mathcal{A}_D$ are the healthy and damaged subdomains, respectively—the aforementioned boundary will then encompass a structural subdomain, $\mathcal{A}_{EZ} \subset \mathcal{A}$, henceforth referred to as an exclusion zone (EZ). The localisation procedure is carried out in a forward manner by postulating one EZ at a time and declaring damage when the replicated field quantity shift matches that induced by damage, which occurs when
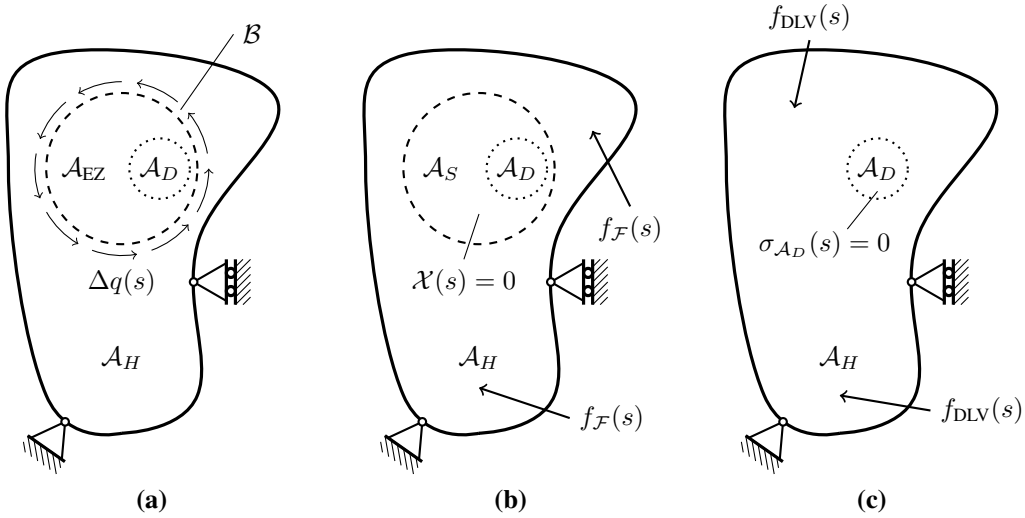
Figure 1: Damage localisation in an n-DOF perturbed structural domain $\mathcal{A} = \mathcal{A}_H \cup \mathcal{A}_D$. (a) SEZ scheme exclusion zone, $\mathcal{A}_{\text{EZ}}$, encompassing damaged subdomain $\mathcal{A}_D$, (b) SDLID scheme cancelling the effect of damage by rendering $\mathcal{A}_S$ dormant, and (c) DDLV scheme revealing the damaged subdomain as that carrying zero stresses

the damaged region is fully contained within a postulated EZ. The scheme utilises a theoretical model to establish a subspace—constituting a basis for all possible shifts in the observed field—by applying linearly independent stress fields to the EZ boundary.

Let $\mathcal{A}$ be discretised with n degrees of freedom (DOF) and subjected to inputs stored in $f(t) \in \mathbb{R}^n$, then the governing equations of motion in the Laplace domain, assuming zero initial conditions, are

$$x(s) = \left(Ms^2 + Cs + K\right)^{-1} f(s) = G(s)f(s) \tag{1}$$

where $M, C, K \in \mathbb{R}^{n \times n}$ are the mass, damping and stiffness matrices, $x(s) \in \mathbb{C}^n$ is the nodal displacement vector, and $G(s) \in \mathbb{C}^{n \times n}$ is the receptance matrix. If a damage is introduced, and the same loading is assumed in both states, we may write

$$\tilde{x}(s) = \tilde{G}(s)f(s) \tag{2}$$

where tilde denotes quantities altered by damage in $\mathcal{A}_D$. Let m measurement DOF be indexed $\mathcal{M} = \{\mathcal{M}_1, \mathcal{M}_2, \ldots, \mathcal{M}_m\}$, we then define the damage-induced shift in displacements as $\Delta x_{\mathcal{M}}(s) = \tilde{x}_{\mathcal{M}}(s) - x_{\mathcal{M}}(s) \in \mathbb{C}^m$.

2.1.1 Reconstruction of the experimental feature using subspace projections

The actual shift in the stress field, $\Delta q(s)$, acting on the EZ boundary, see Figure 1a, is not known. We instead operate with a subspace, $W(s) \in \mathbb{C}^{m \times b}$, constituting a basis for all possible differences in the observed field obtained from b linearly independent stress fields acting on the EZ boundary, comprised of DOF indexed as $\mathcal{B} = \{\mathcal{B}_1, \mathcal{B}_2, \ldots, \mathcal{B}_b\}$. As such,

$$\Delta x_{\mathcal{M}}(s) = W(s)\Delta q(s) \tag{3}$$

3

As implied earlier, multiple EZs are employed during structural damage interrogation. For generality, we employ z EZs, indexed by $y \in [1, z]$. Let $\Delta \hat{q}^{(y)}(s)$ be the least squares estimator computed for the yth EZ as

$$\Delta \hat{q}^{(y)}(s) = \operatorname*{argmin}_{\Delta \hat{q}^{(y)}(s)} \| \Delta x_{\mathcal{M}}(s) - W^{(y)}(s) \Delta \hat{q}^{(y)}(s) \| = W^{(y)^{\dagger}}(s) \Delta x_{\mathcal{M}}(s) \tag{4}$$

from which the Moore-Penrose pseudoinverse $W^{(y)^{\dagger}}(s)$ exists when rank $\left(W^{(y)}(s) \right) = b$, thus imposing the restriction on the scheme $m > b$. From Equations (3) and (4), a residual may be computed as

$$\epsilon^{(y)}(s) = \left(I - W^{(y)}(s) W^{(y)^{\dagger}}(s) \right) \Delta x_{\mathcal{M}}(s) \tag{5}$$

for which the singular value, $\varsigma^{(y)}$, is determined. Damage may then be declared in EZ k if $\forall y \neq k : \varsigma^{(k)} < \varsigma^{(y)}$.

2.2 The SDLID scheme

The SDLID scheme operates by shaping multiple inputs—using a theoretical model of the reference structure—such that certain vibration quantities in a postulated structural subdomain, $\mathcal{A}_S \subset \mathcal{A}$, are rendered dormant. Damage is then located by applying these shaped inputs to the system, both in the reference and damaged state, and when $\mathcal{A}_S \supseteq \mathcal{A}_D$, the measured field quantity will, in theory, be identical in the two states. The interrogation is, in analogy to the SEZ scheme, carried out by considering one structural subdomain at a time. This scheme operates without system identification and it can, in principle, operate by deploying just one well-placed output sensor.

2.2.1 Shaping of controllable inputs

In this paper, the inputs are shaped in the Laplace domain, which is feasible as the inputs considered are exclusively harmonic. The task of shaping these inputs is briefly explained.

Consider the system depicted in Figure 1b discretised with n DOF and assume vibration in steady-state induced by r controllable inputs acting in DOF indexed by $\mathcal{F} = \{\mathcal{F}_1, \mathcal{F}_2, \ldots, \mathcal{F}_r\}$. If interrogation is conducted over e structural subdomains, indexed by $g \in [1, e]$, we get

$$x^{(g)}(s) = G_{\bullet, \mathcal{F}}(s) f_{\mathcal{F}}^{(g)}(s) \tag{6}$$

where $G_{\bullet, \mathcal{F}}(s) \in \mathbb{C}^{n \times r}$ contains the columns of the receptance matrix corresponding to the input DOF and $f_{\mathcal{F}}^{(g)}(s) \in \mathbb{C}^r$ contains the shaped inputs. If each structural subdomain, $\mathcal{A}_S^{(g)}$, is comprised of v quantities we seek to suppress, then by introducing a transformation matrix, $T^{(g)} \in \mathbb{R}^{v \times n}$, we write

$$\mathcal{X}^{(g)}(s) = T^{(g)} x^{(g)}(s) \tag{7}$$

where $\mathcal{X}^{(g)}(s) \in \mathbb{C}^v$ is a linear combination of the DOF sought to suppress. The transformation matrix, T, allows for extraction of the desired DOF as well as mapping these to, for example, strains (11). Substituting Equation (6) into Equation (7) provides

$$\mathcal{X}^{(g)}(s) = T^{(g)} G_{\bullet, \mathcal{F}}(s) f_{\mathcal{F}}^{(g)}(s) \tag{8}$$

4

and we see that $f_{\mathcal{F}}^{(g)}(s)$ yields $\mathcal{X}^{(g)}(s) = 0$ if

$$f_{\mathcal{F}}^{(g)}(s) = \ker(T^{(g)} G_{\bullet,\mathcal{F}}(s)) \tag{9}$$

hence imposing the following restriction on the scheme: $r > v$.

After input shaping, the procedure is to apply these inputs to the actual structure in its reference state and its damaged one to extract the field quantity shift $\Delta x_{\mathcal{M}}^{(g)}(s) = \tilde{x}_{\mathcal{M}}^{(g)}(s) - x_{\mathcal{M}}^{(g)}(s)$. The damage metric employed in this paper is the ℓ^2-norm of the shift, which we denote $\psi^{(g)}$. Damage may now be declared in subdomain w if $\forall g \neq w : \psi^{(w)} < \psi^{(g)}$.

2.3 The DDLV scheme

The premise of the DDLV scheme is to locate stiffness-related damage by inspecting stress fields computed in a model using load vectors from the kernel of estimated transfer matrix shifts. More specifically, the undamaged and damaged system transfer matrices are estimated experimentally, and from their shift, null vectors are extracted. These are then applied as loading to a theoretical model, revealing damaged regions as those carrying zero stresses, $\sigma_{\mathcal{A}_D}(s) = 0$, as illustrated in Figure 1c. An obvious drawback of this scheme—compared to the other two—is the imminent call for system identification in order to establish approximations of the transfer matrices. In contrast to the other two, however, no specific domain is interrogated at one time, which ensures that multiple damaged regions may be located.

The experimental transfer matrices from the undamaged and damaged states of the structure, $G_e(s)$ and $\tilde{G}_e(s)$, are mapped from m outputs and r independent inputs, thereby leading to $G_e(s) \in \mathbb{C}^{m \times r}$. We assume throughout this paper that at least one input and output are collocated, which lets us define the transfer matrices over the union of input and output coordinates, $\mathcal{U} = \mathcal{F} \cup \mathcal{M}$ (13). This scheme does not call on any assumptions regarding the input (except for adhering to typical modal analysis conditions).

2.3.1 Derivation of the damage locating vector

The DDLV theorem states that the kernel of $\Delta G_e(s) = \tilde{G}_e(s) - G_e(s)$ contains vectors with damage locating properties. If $\mathrm{rank}(\Delta G_e(s)) < \#\mathcal{U}$, we get

$$f_{\mathcal{U}}(s) = \ker(\Delta G_e(s)) \tag{10}$$

from which the damage locating vector is computed as

$$f_{\mathrm{DLV}}(s) = K G_{\bullet,\mathcal{U}}(s) f_{\mathcal{U}}(s) \tag{11}$$

Letting the theoretical model be discretised with c elements indexed by $d \in [1, c]$, we can compute the individual element forces by employing $f_{\mathrm{DLV}}(s)$ as loading in a static context. The damage metric employed for this scheme is the ℓ^2-norm of the element forces, denoted $\vartheta^{(d)}$, and damage is then declared in element o if $\forall d \neq o : \vartheta^{(o)} < \vartheta^{(d)}$.

3. Damage localisation with introduced model discrepancy

As previously noted, the purpose of this paper is to assess how the SEZ scheme performs when tasked with locating damage while facing model discrepancy. The performance of the SDLID and DDLV schemes is concurrently evaluated to gain perspective. In order to gain a more elaborate understanding of this type of discrepancy, we choose to divide the study into two subcategories of model discrepancy, both of which are expected to be present in practice. The first study explores the sensitivity of the schemes with regard to discretisation discrepancy, while the second study investigates the robustness to model parameter discrepancy. As this paper is solely devoted to investigate robustness to model errors, ambient noise is excluded from the studies.

The finite element models established in this study are comprised of planar Bernoulli-Euler beam elements, see Figure 2. The models have a width and height of 3 m. An isotropic material model is assigned and the material parameters resemble those of generic structural steel with the modulus of elasticity taken as $E = 200$ GPa, the mass density as $\rho = 7850$ kg/m^3 and Poisson's ratio of $\nu = 0.3$. The damping is defined as mass proportional with 5 % damping in the first mode. Two models of different discretisation are established, which we will refer to as Model A (Figure 2a), discretised with 38 elements, and Model B (Figure 2b), discretised with 19 elements. The eigenfrequencies of these models are presented in Table 1 to show the discrepancy-induced shifts.

As previously stated, two classifications of model errors are adopted in this study, namely, discretisation discrepancy and model parameter discrepancy. In both cases, we choose to investigate the localisation outcome of 17 damage scenarios, ranging from damage in a structural subdomain corresponding to element 3 (Model B) to damage in a structural subdomain corre-
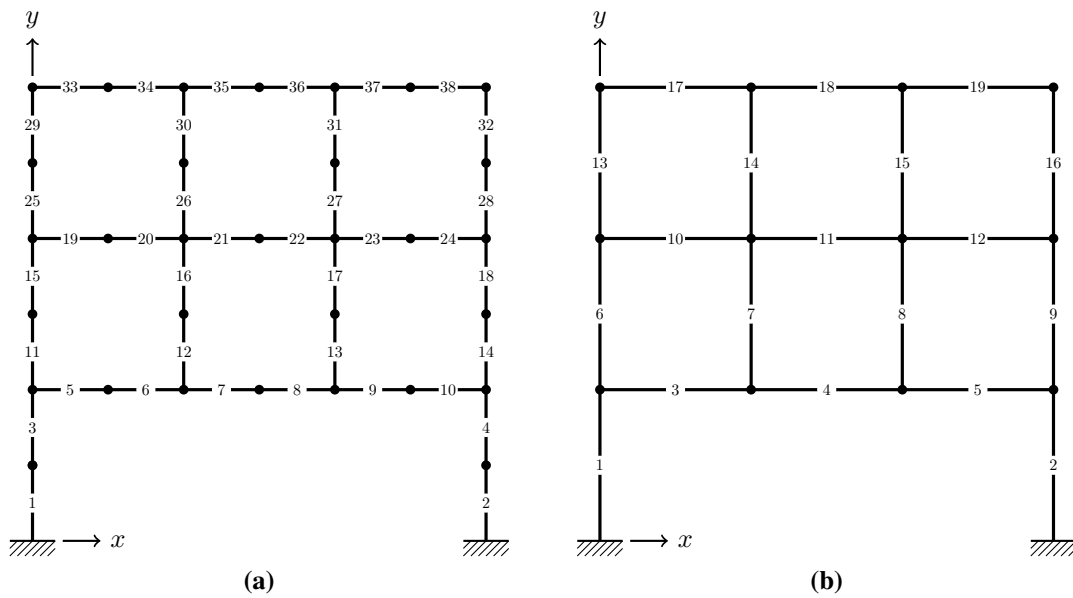

(a)   (b)

Figure 2: **Element numbering of (a) Model A and (b) Model B, where (●) denotes nodes**

Table 1: First five undamped angular eigenfrequencies of Models A and B

Eigenmode	Eigenfrequency (Model A) (rad/s)	Eigenfrequency (Model B) (rad/s)
1	55.13	55.14
2	153.8	154.1
3	196.0	196.3
4	338.3	339.8
5	368.5	369.2
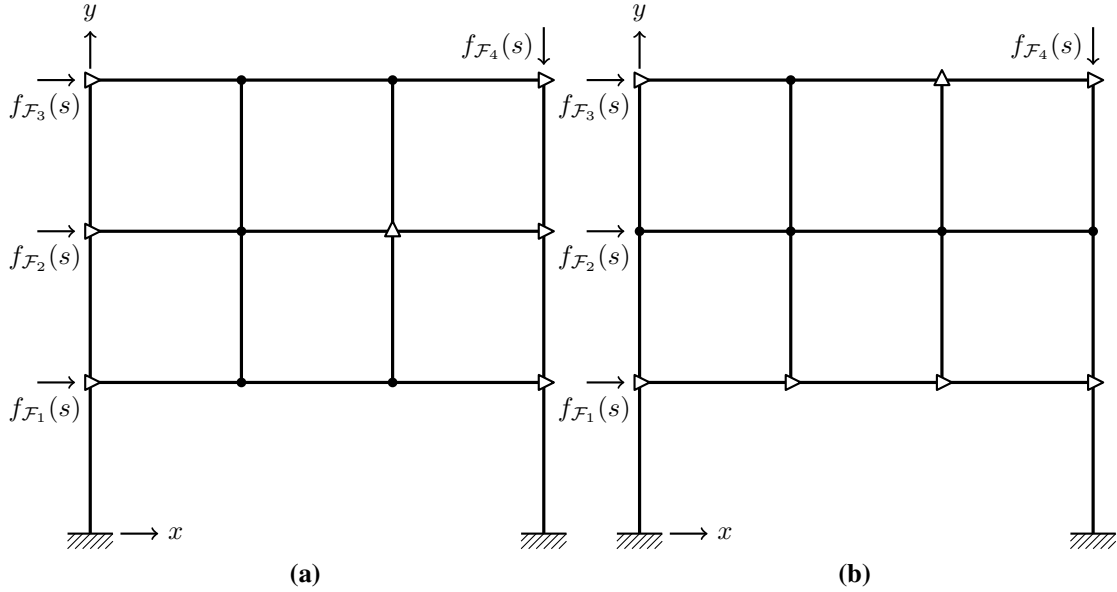
Figure 3: Input/output configurations (a) B and (b) C, where ($\bullet$) denotes nodes, ($\triangleright$) denotes sensors measuring in the x-direction and ($\triangle$) denotes sensors measuring in the y-direction

sponding to element 19. We introduce damage as a 1 % reduction of the modulus of elasticity of the subdomain related to the specific damage scenario, thereby ensuring that the damage-induced eigenfrequency shift is smaller than the discrepancy-induced shift. Each scenario is tested for a subset of ten interrogation frequencies, $\mathcal{S} = \{10j, 30j, 40j, 70j, 90j, 100j, 125j, 230j, 260j, 290j\}$, which are selected such that they do not conflict with any eigenfrequencies, as suggested by Bernal in (12). Furthermore, we set out to test for different input/output configurations, of which three are included in this paper. The first configuration, which we will denote Configuration A, consists of sensors measuring in all DOF (a total of 36) of Model B and inputs distributed as shown in Figure 3. The second and third configuration — dubbed Configurations B and C, respectively — constitute subsets with 7 sensors from Configuration A. These are shown in Figure 3.

3.1 Discretisation discrepancy

The first study will treat the inevitable discretisation discrepancy that will arise between real, continuous structures and discrete mathematical models. This discrepancy is ensured by employing Model A to represent the structure in the reference and damaged states (referred to as the truth models), and letting the coarser discretised Model B take the place of the theoretical model. 17 damage scenarios are considered in this case. Damage is introduced to a span of elements in Model A that correspond to one element of Model B. For example, damage scenario 1 is a reduction of the modulus of elasticity of elements 5 and 6 in Model A, which correspond to element 3 in Model B. We tune Model B such that the eigenfrequency closest to the interrogation frequency, $\mathcal{S}_i$, matches that of Model A in reference state. A total of 170 simulations are run for each input/output configuration, of which the probability of localisation (POL) is shown in Figure 4. Here, the POL is simply taken as the percentage of right damage location classifications.

It is evident that the DDLV scheme performs better than the SEZ and SDLID schemes, albeit marginally. The reason that the DDLV scheme pulls ahead may be attributed to the fact that it relies on a statically generated stress field to localise damage, which, in itself, should be more robust to errors than the dynamic contexts in which the SEZ and SDLID schemes operate.
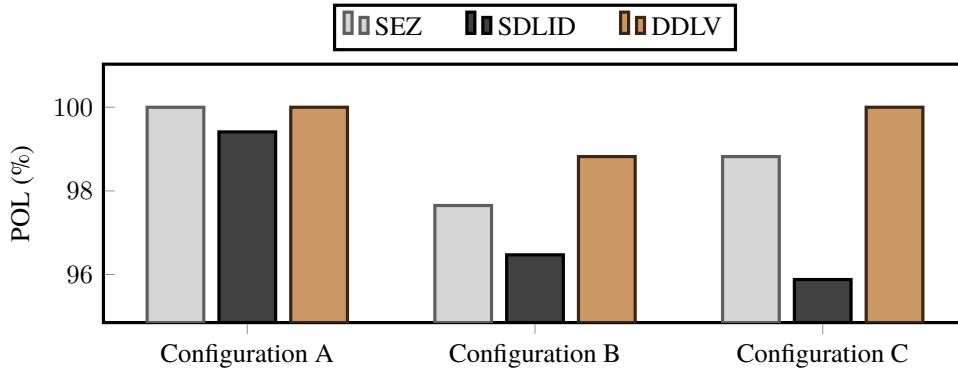

Figure 4: POL when discretisation discrepancy is introduced

3.2 Parameter discrepancy

We seek to evaluate how the schemes perform when presented with discrepancy between model parameters. We now take Model B to represent both the truth models as well as the theoretical model. Discrepancy between the truth models and the theoretical model is introduced by assigning different values of the modulus of elasticity to each element in the truth models. These values are drawn from a uniform distribution, which we denote $U((1-\alpha)E, (1+\alpha)E)$, where α is a measure of the discrepancy. 17 damage scenarios are again considered, comprising perturbations of the modulus of elasticity of elements 3 through 19 in Model B. A total of 1700 simulations are run for each input/output configuration at each level of discrepancy.
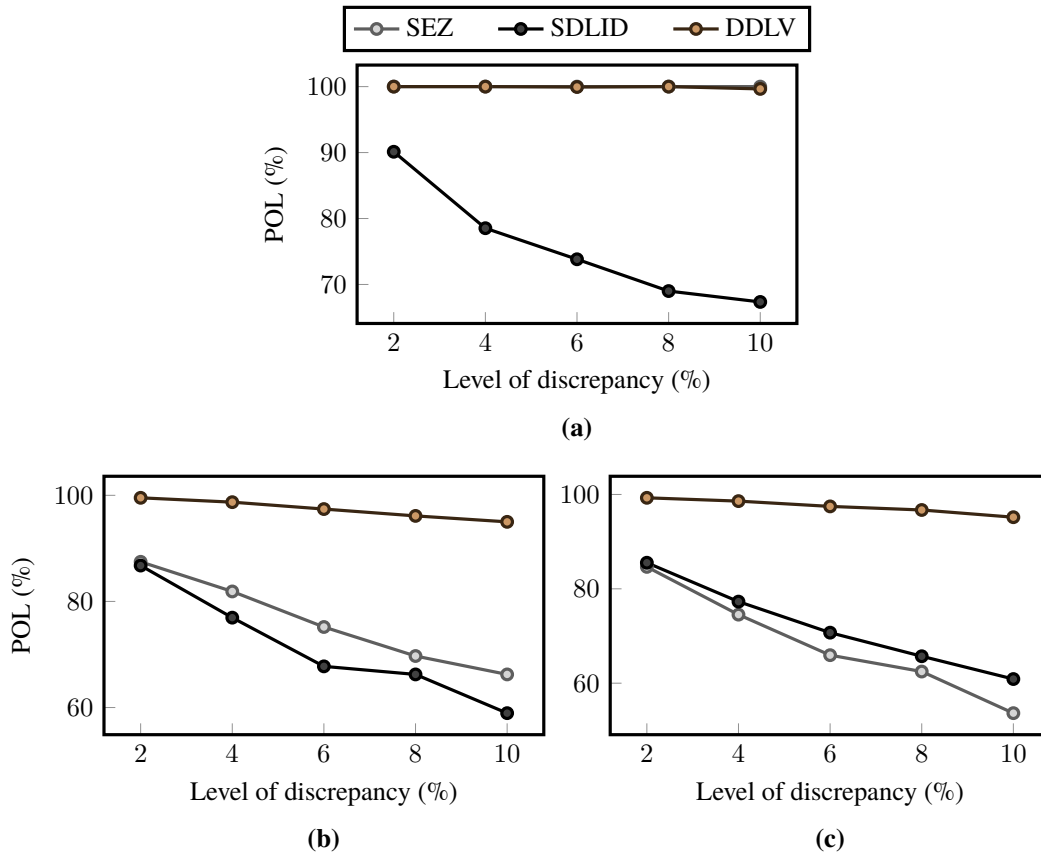
8

Figure 5: Relationship between POL and increased parameter discrepancy for (a) Configuration A, (b) Configuration B and (c) Configuration C

We once again tune the eigenfrequencies of the theoretical model to match those of the truth model in reference state.

The POL for all configurations are illustrated in Figure 5 for five levels of discrepancy. Although the SEZ and DDLV schemes are on par when a full set of sensors is deployed, the SEZ scheme demonstrates less robustness when more realistic sensor distributions are tested. The high level of robustness of the DDLV scheme is once again attributed to the fact that it relies on the theoretical model for static analysis.

4.   Conclusion

Numerical simulations show that, when faced with discretisation discrepancy, the performance of the SEZ, SDLID and DDLV schemes were nearly tantamount, suggesting that the SEZ and SDLID schemes would not be more sensitive to model error than the DDLV. But, as model errors generally appear as a combination of the discretisation and parameter discrepancies, the second study established that the theoretical model of the DDLV scheme is, in fact, more robust to the model errors considered in this paper. It is important to note, however, that as ambient noise is excluded from these findings, they do not necessarily reflect general

robustness of the schemes.

References

1. L Mevel, L Hermans and HV Auweraer, "Application of a subspace-based fault detection method to industrial structures", Mech. Syst. Sig. Process. 13(6), pp 823–838, 1999.
2. MD Ulriksen, D Tcherniak and L Damkilde, "Damage detection in an operating vestas v27 wind turbine blade by use of outlier analysis", IEEE 2015 EESMS Conf. Proc., pp 50–55, 2015.
3. D Tcherniak and LL Mølgaard, "Active vibration-based structural health monitoring system for wind turbine blade: Demonstration on an operating vestas v27 wind turbine", Struct. Health Monitor. 16(5), pp 536–550, 2017.
4. S Gres, MD Ulriksen, M Döhler, RJ Johansen, P Andersen, L Damkilde and SA Nielsen, "Statistical methods for damage detection applied to civil structures", Proc. Eng. 199, pp 1919–1924, 2017.
5. CR Farrar and K Worden, Structural Health Monitoring: A Machine Learning Perspective, John Wiley & Sons, Inc., 2013.
6. MD Ulriksen, Damage Localization for Structural Health Monitoring: An Exploration of Three New Vibration-based Schemes, Ph.D. thesis, Aalborg University, 2018.
7. SW Doebling, CR Farrar and MB Prime, "A summary review of vibration-based damage identification methods", The Shock Vib. Digest 30(2), pp 91–105, 1998.
8. CP Fritzen, "Vibration-based structural health monitoring – concepts and applications", Key Eng. Mat. 293-294, pp 3–20, 2005.
9. CR Farrar, SW Doebling, PJ Cornwell and EG Straser, "Variability of modal parameters measured on the alamosa canyon bridge", SPIE Proc. - The International Society for Optical Engineering 1, 1997.
10. D Bernal and MD Ulriksen, "Subspace exclusion zones for damage localization", Mech. Syst. Sig. Process. (In press), 2018.
11. MD Ulriksen, D Bernal and L Damkilde, "Shaped input distributions for structural damage localization", Mech. Syst. Sig. Process. 110, pp 499–508, 2018.
12. D Bernal, "Damage localization from the null space of changes in the transfer matrix", AIAA J. 45(2), pp 374–381, 2007.
13. D Bernal and O Tigli, "On the analytical expansion of transfer matrices", IMAC XXIV Conf. Proc., 2006.